

# Controllable Layered Image Generation for Real-World Editing

Jinrui Yang<sup>1,2,\*</sup> Qing Liu<sup>2</sup> Yijun Li<sup>2</sup> Mengwei Ren<sup>2</sup>  
 Letian Zhang<sup>1</sup> Zhe Lin<sup>2</sup> Cihang Xie<sup>1</sup> Yuyin Zhou<sup>1</sup>  
<sup>1</sup>UC Santa Cruz <sup>2</sup>Adobe Research

<https://rayjryang.github.io/LASAGNA-Page/>

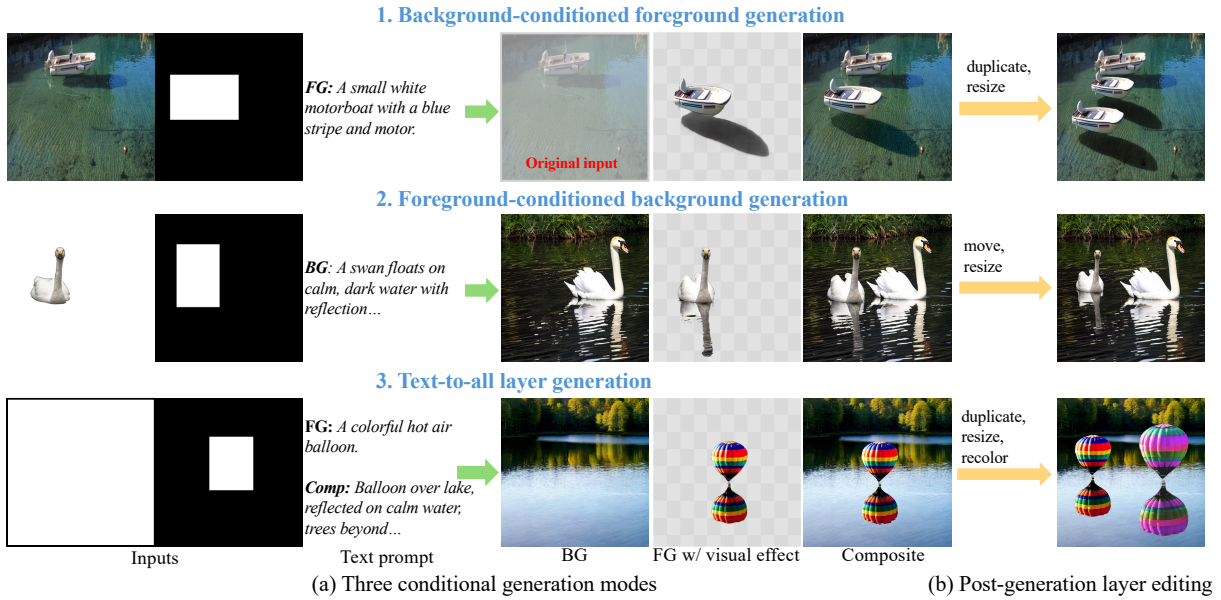


Figure 1. **Layered generation with LASAGNA.** (a) Our framework supports three generation modes: background-conditioned foreground generation, foreground-conditioned background generation, and text-to-all layer generation, which flexibly handle different inputs and jointly synthesize coherent, high-quality composites, backgrounds, and transparent foregrounds with realistic visual effects (e.g., shadows and reflections). (b) Generated layers enable direct post-editing into new, coherent scenes.

## Abstract

Recent image generation models have shown impressive progress, yet they often struggle to yield controllable and consistent results when users attempt to edit specific elements within an existing image. Layered representations enable flexible, user-driven content creation, but existing approaches often fail to produce layers with coherent compositing relationships, and their object layers typically lack realistic visual effects such as shadows and reflections. To overcome these limitations, we propose LASAGNA, a novel, unified framework that generates an image jointly with its composing layers—a photorealistic background and a high-quality transparent foreground with compelling visual effects. Unlike prior work, LASAGNA efficiently learns correct image composition from a wide range of conditioning inputs—text prompts, foreground, background, and location masks—offering greater controllability for real-world applications. To enable this, we introduce LASAGNA-48K, a new dataset composed of clean backgrounds and RGBA foregrounds

with physically grounded visual effects. We also propose LASAGNA BENCH, the first benchmark for layer editing. We demonstrate that LASAGNA excels in generating highly consistent and coherent results across multiple image layers simultaneously, enabling diverse post-editing applications that accurately preserve identity and visual effects. LASAGNA-48K and LASAGNA BENCH will be publicly released to foster open research in the community. The project page is <https://rayjryang.github.io/LASAGNA-Page/>.

## 1. Introduction

Recent advances in text-to-image generation have predominantly leveraged diffusion-based generative models, enabling impressive synthesis quality and semantic accuracy from text prompts [11, 24, 35, 39, 43, 53]. Despite their success, these models typically produce images as a single entity, limiting controllability for

\*This work was done when Jinrui Yang was a research intern at Adobe Research.

real-world editing tasks. Consequently, modifications to individual elements within a generated image—such as repositioning, scaling, or adjusting a specific object—often require complex prompt engineering or re-generating the entire image, making it difficult to preserve desired attributes in other regions.

To achieve controllable editing, recent works [8, 17, 61, 68] explore compositional and layered image generation. This approach, which decomposes generated images into layers, allows for independent manipulation of image components. However, current layered approaches fall short in several critical aspects that prevent their use in real-world scenarios:

1. The faithful generation of visual effects like shadows and reflections intrinsically associated with the foreground object is largely overlooked.
2. Current approaches often lack a unified framework capable of handling diverse conditional inputs such as foreground, background, masks, text, therefore limiting their controllability and practical utility.
3. As shown in Table 1, most existing methods rely on proprietary or non-public training data. Public datasets like MULAN[45] still fall short, as they lack realistic foreground visual effects essential for downstream editing. Moreover, the absence of standardized evaluation protocols further hinders meaningful progress comparison across studies.

In this work, we address these limitations and enable controllable, versatile, and realistic layered editing from three complementary perspectives: a unified generation paradigm, publicly available training data, and a standardized benchmark. We present LASAGNA, a novel framework designed to generate images as a composition of foreground layers and background layers, explicitly embedding visual effects such as shadows and reflections. This unified architecture simultaneously integrates diverse conditioning inputs and supports three generation modes: background-conditioned foreground layer generation (**FG\_Gen**), foreground-conditioned background generation (**BG\_Gen**), and text-to-all layer generation (**Text2All**). In **BG\_Gen**, LASAGNA further restores the foreground’s missing visual effects while preserving its identity, enabling the resulting foreground layer to remain fully editable in subsequent operations.

To enable LASAGNA training, we introduce LASAGNA-48K, a new dataset of 48K natural images with faithfully decomposed RGBA foreground and background layers. Critically, these foregrounds accurately preserve effects like shadows and reflections in relation to the object and its transparency. We will release LASAGNA-48K to facilitate the research and development of models capable of capturing these complex, physically-based interactions.

Furthermore, we introduce LASAGNABENCH to establish a standardized measure for our method and future research. Evaluation in layer editing and generation has been challenging, as prior work relies on be-

Table 1. **Layer Dataset Overview.** ✓: available; ×: not available or non-public.

Paper	Layer data (Public)	Eval Bench	Visual Effect
MULAN [45]	✓ (✓)	×	×
LayerDiffuse [61]	✓ (×)	×	×
PSDiffusion [17]	✓ (×)	×	×
LASAGNA(ours)	✓ (✓)	✓	✓

spoke protocols and user studies. LASAGNABENCH provides the first public benchmark for this task, featuring 242 real-world images sourced from six diverse datasets, each meticulously decomposed by human experts into high-fidelity, text-paired layers that accurately capture complex visual effects. On LASAGNABENCH, our method achieves superior layer generation while preserving object identity, spatial fidelity, and visual coherence.

In summary, our primary contributions are:

- We present **LASAGNA**, a unified framework supporting three generation modes and flexible conditioning inputs (text, images, masks). It synthesizes realistic composite images by jointly or individually generating coherent backgrounds and RGBA foregrounds with visual effects, enabling highly controllable, professional photo-editing-tool-style image editing without additional model inference.
- A new dataset **LASAGNA-48K**, featuring over 48K natural images with decomposed background layers as well as foreground layers with physically-grounded visual effects.
- **LASAGNABENCH**, the first public benchmark for rigorous and standardized evaluation of controllable layer-based generation and editing.
- Our method delivers high-quality layer generation and editing, especially for tasks requiring strict identity preservation and harmonious integration.

## 2. Related works

### 2.1. Text-to-Image and Image Editing Models

Recent text-to-image diffusion models [11, 24, 35, 39, 43, 53] have made remarkable progress in generating high-fidelity images from text. However, these models are typically confined to single-layer synthesis, lacking an explicit layered representation. Consequently, they cannot produce RGBA outputs or support independent post-generation editing of specific elements without unintended changes to other regions. While specialized image editing models [6, 24, 29, 53, 62, 66, 68] have been developed for common editing tasks, they still struggle with precise object-level control and often introduce non-local artifacts. They are particularly weak in complex spatial edits, such as enlarging or relocating an object while preserving its identity and appearance, as they lack an understandings of the layered composition of the scene. This motivates the development of layer-centric frameworks that inherently

support structured, controllable synthesis and editing.

## 2.2. Image Layer Generation

To enable compositional editing, prior work has explored two main paradigms for layered generation.

(1). **Image-layer extraction via post processing:** This common pipeline first uses text-to-image models [11, 24, 35, 39, 43, 53] to generate an RGB composite image. Then, existing segmentation models [22, 41, 42] can be used to extract an independent foreground layer. Finally, inpainting models (e.g., [19, 50, 51, 67, 70]) are typically employed to reconstruct the occluded background. However, this multi-stage, separately optimized pipeline accumulates errors across stages and often fails to preserve global coherence and cross-layer consistency during post-editing. Operations such as object translation or scaling often produce spatially inconsistent or visually unnatural results.

(2). **Direct transparent image layer generation:** This paradigm aims to generate layers directly. Some methods [12, 61] generate RGBA layers directly from text but often target simple scenes and fail to capture complex interactions between objects and surrounding context, leading to noticeable realism gaps. Other methods, such as LayerDecomp [56], can extract foreground layers with realistic visual effects but lack the ability to generate novel foreground content, thereby limiting their applicability. Multi-layer generation methods like LayerDiffusion [61] and LayerFusion [8] employ separate models [35, 61], which lack a unified control mechanism and struggle with consistency. PSDiffusion [17] supports text-to-multilayer generation but lacks conditional synthesis capabilities, essential for many real-world editing workflows.

Crucially, none of these methods provide a unified, controllable generation framework that enables generating transparent foregrounds with physically-grounded visual effects. Our LASAGNA framework aims to address this key barrier to real-world editing.

## 2.3. Layer Dataset

Previous studies [17, 20, 45, 64] have introduced several layer-related datasets. MULAN [45], a prominent multi-layer dataset, provides object-level decompositions but does not include explicit visual effects as part of the foreground layers. Text2Layer [64] generates a two-layer decomposition, but the dataset is not public and does not incorporate visual effects. PSDiffusion [17] propose an internal multi-layer dataset, consisting of 30K samples. Except for MULAN, most datasets remain private and none explicitly account for visual effects. To bridge this data gap, we introduce LASAGNA-48K, a new dataset built upon an advanced decomposition model that jointly generates background and foreground layers while faithfully preserving complex visual effects in the foreground’s alpha channel. In addition, we manually annotate a

Table 2. Overview of the three generation modes.

Mode	Inputs	Targets
FG_Gen	$\{c_{\text{txt}}, c_{\text{mask}}, c_{\text{bg}}\}$	$\{x_0^{\text{comp}}, x_0^{\text{fg+ve}}\}$
BG_Gen	$\{c_{\text{txt}}, c_{\text{mask}}, c_{\text{fg}}\}$	$\{x_0^{\text{comp}}, x_0^{\text{bg}}, x_0^{\text{fg+ve}}\}$
Text2All	$\{c_{\text{txt}}, c_{\text{mask}}\}$	$\{x_0^{\text{comp}}, x_0^{\text{bg}}, x_0^{\text{fg+ve}}\}$

high-quality layer benchmark. All training and testing data are fully released to encourage transparency and foster further research in this area.

## 3. Approach

### 3.1. LASAGNA Framework

As shown in Fig. 2, LASAGNA models the joint generation of composite images  $x^{\text{comp}}$ , backgrounds  $x^{\text{bg}}$ , and foregrounds with visual effects  $x^{\text{fg+ve}}$  as a flexible, layer-conditional denoising task. Our model learns to denoise a set of target images  $\mathbf{X}_t \subseteq \{x_t^{\text{comp}}, x_t^{\text{bg}}, x_t^{\text{fg+ve}}\}$  conditioned on a set of inputs  $\mathbf{C} \subseteq \{c_{\text{txt}}, c_{\text{mask}}, c_{\text{bg}}, c_{\text{fg}}\}$ . By varying the composition of  $\mathbf{X}_t$  and  $\mathbf{C}$ , we unify three generation modes (FG\_Gen, BG\_Gen, and Text2All) in a single model, addressing different real-world editing needs (see Table 2).

We build LASAGNA upon the Diffusion Transformer (DiT) architecture [6, 34] to support flexible editing tasks, adapted to handle heterogeneous inputs. We employ four embedding types to distinguish between different tasks and image types:

- *Type Embedding*—represents the semantic role of each image, e.g., background or foreground.
- *IO Embedding*—indicates whether a frame is used as an input or an output in the current task.
- *Position Embedding*—spatial position of image tokens.
- *Timestep Embedding*—the diffusion step.

Meanwhile, text prompts are processed into tokens by a T5 encoder [38]. All conditional tokens and noisy target tokens are then concatenated into a single sequence, allowing the model’s self-attention blocks to seamlessly integrate information from any arbitrary set of conditions  $\mathbf{C}$  to guide the denoising of targets  $\mathbf{X}_t$ .

We train our model by optimizing a unified denoising objective across all conditional generation tasks. Each mode uses its specific conditional inputs  $\mathbf{C}^{(m)}$  and targets  $\mathbf{X}_0^{(m)}$  as defined in Table 2. The model is trained to minimize the joint expectation  $\mathcal{L}_{\text{dm}}$  over this multi-task distribution:

$$\mathcal{L}_{\text{dm}} = \mathbb{E}_{m,t,\mathbf{X}_0^{(m)},\epsilon} \left[ \|\epsilon_{\theta}(\mathbf{X}_t^{(m)}; \mathbf{C}^{(m)}, t) - \epsilon\|_2^2 \right]$$

$$\text{s.t. } \mathbf{X}_t^{(m)} = \sqrt{\alpha_t} \mathbf{X}_0^{(m)} + \sqrt{1 - \alpha_t} \epsilon, \text{ and } \epsilon \sim \mathcal{N}(\mathbf{0}, I).$$

The training loss follows flow matching [27].

### 3.2. LASAGNA-48K Dataset

To enable the training of our controllable, layer-based framework, we introduce LASAGNA-48K, a large-

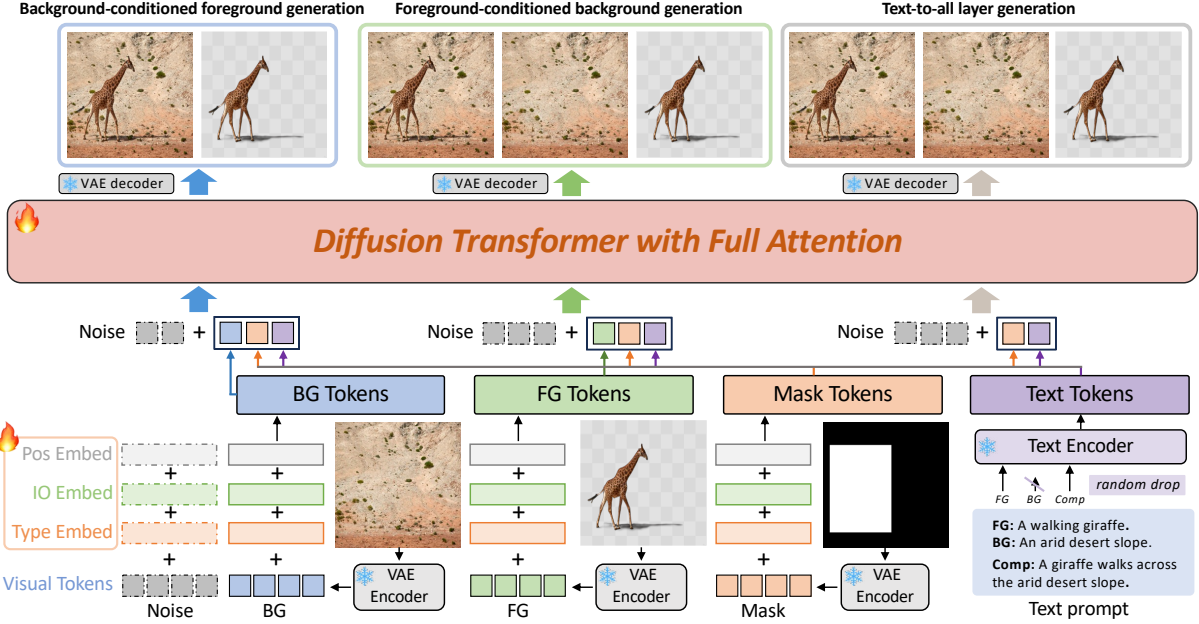


Figure 2. **Pipeline of LASAGNA framework.** We formulate the joint generation of composite images, backgrounds, and foregrounds as a flexible, layer-conditional denoising task. This single framework supports multiple workflows, including FG\_Gen, BG\_Gen, and Text2All. We use a unified input representation with learnable embeddings that distinguish different roles of visual latents (noise, BG, FG, and mask) across tasks, enabling the model to adapt its behavior under various generation settings. This allows a single attention-based model to flexibly process varied combinations of inputs and targets simultaneously.

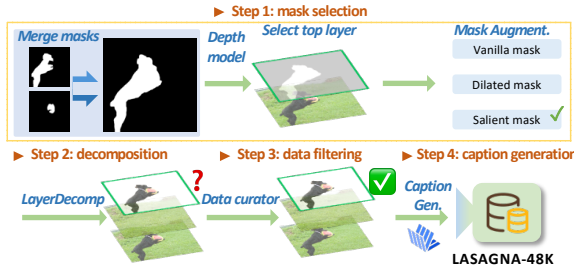


Figure 3. **Data construction pipeline.** Starting with existing datasets, we implement a four-stage data construction pipeline leveraging off-the-shelf models with a custom-trained data curator. This process yields a high-quality dataset as the foundation for subsequent model training.

scale dataset of over 48K high-quality image triplets.

**Data sources.** We construct our dataset by curating samples from three public sources: MULAN [45], COCO 2017 [26], and SOBA [48]. MULAN provides existing layered representations but lacks visual effects. COCO offers a vast diversity of real-world scenes with complex object layouts, essential for learning robust editing capabilities. SOBA, originally a shadow detection dataset, provides rich examples of realistic visual effects, offering valuable supervision for realistic composite generation. The final dataset comprises 8K samples from MULAN, 39K from COCO, and 1K from SOBA.

**Data construction pipeline.** We design a four-stage pipeline to ensure high data fidelity as shown in Fig. 3: 1. *Non-occluded mask selection*. To ensure robust

downstream results, each object comes with multiple mask variants. We create vanilla masks for foremost objects using layer annotations (for MULAN) and instance annotations with depth estimation [21] (for COCO). We extract salient masks with a salient segmentation model [13], highlighting most prominent regions within objects. We also produce dilated masks with morphological operations.

2. *LayerDecomp decomposition*. We process each image and its mask variants with LayerDecomp [56], extracting multiple sets of backgrounds and foregrounds with visual effects.
3. *Data filtering*. We observe that the quality of backgrounds and foregrounds extracted from LayerDecomp is strongly correlated. We train a data curator built upon InternVL2.5-8B [7] to assess the backgrounds fidelity and filter low-quality data. The curator is trained on 30K carefully annotated samples (see Appendix), and achieves 88.8%/72.3% precision/recall on a held-out test set. After filtering, we further use Qwen2.5-VL-32B [1] to remove residual artifacts in foregrounds.
4. *Captioning*. After obtaining high-quality triplets of composite images, backgrounds, and foregrounds, we prompt InternVL 2.5-38B [7] to caption these images jointly, considering cross-image relationships for semantically consistent descriptions.

See Fig. 4 for example of generated training data in the form of image triplets and captions.

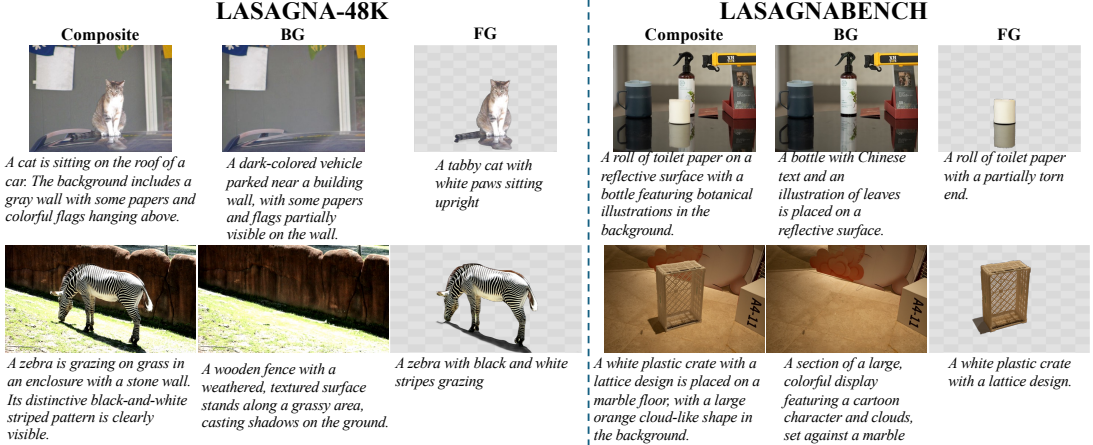


Figure 4. **Samples of LASAGNA-48K and LASAGNABENCH.** Each sample consists of a composite image, a clean background, and a foreground layer with visual effects, along with corresponding captions for all components.

Table 3. **Benchmark statistics.** LASAGNABENCH is built from 6 distinct sources—four public datasets [26, 45, 46, 48] and two in-house data—to ensure diversity and representativeness.

Data Source	#	Data Source	#	Data Source	#
MULAN	45	COCO 2017	40	SOBA	50
Unsplash	27	Camera-Indoor	40	Camera-Outdoor	40

## 4. Experiments

**LASAGNA Implementation.** We finetune a pre-trained 2B-parameter DiT model. All conditional images and targets are encoded with RGBA-VAE, which is finetuned from DiT VAE using a combination of L1, GAN, and perceptual losses [63]. We adopt resolution-specific batching (batch size 6 for  $512^2$  resolution, 1 for  $1024^2$ ) to improve generalization across scales. We use the AdamW optimizer and set the learning rate to  $1.2 \times 10^{-5}$  with linear warm-up for  $2K$  steps. The model is trained for 20K iterations. For inference, results are generated using DDIM sampling for 50 steps.

### 4.1. Benchmark

We introduce LASAGNABENCH, the first publicly available benchmark specifically designed for layer-centric image generation. Prior works [8, 17, 61] employ differing evaluation protocols on non-public datasets. To address this, we build LASAGNABENCH comprising 242 samples sourced from 6 diverse datasets: 4 public sources [26, 45, 46, 48] and 2 in-house data sources, all of which will be released (summarized in Table 3 and Fig. 4). Each sample consists of a real photographic composite image, a background image, a foreground with visual effects annotated by professional annotators, and descriptive captions. For public datasets, backgrounds were generated with LayerDecomp, followed by automated curation and manual verification to ensure consistency. For in-house datasets, we captured controlled real-world

photography pairs (before and after object removal), following a similar data collection methodology as in prior works [51, 56]. These collection efforts ensure that LASAGNABENCH offers a diverse and high-quality set of layer representations, capturing realistic variations in object appearance and surrounding background scenes, along with physically grounded visual effects.

### 4.2. Layer Generation vs General Models

We compare LASAGNA with three leading image generation and editing models: FLUX.1 [18, 24], Qwen-Image [53], and gpt-image-1[high] [31]. Since these models do not natively support multi-task generation, we employ their task-specific variants (e.g., inpainting/editing models for conditional tasks, T2I models for Text2All) to ensure fair comparison at their best performance. Because these baselines also lack multi-layer generation capability, we focus evaluation on the generated composite images. We employ FID [16, 33] and CLIP-FID [33] to measure image quality and semantic alignment. Following Complex-Edit [57], we also use a GPT-4o-based score to evaluate Instruction Following and Identity Preservation, averaging them into a final score of 0 to 10.

As shown in Table 4, LASAGNA consistently outperforms existing methods across all three generation modes, achieving higher image quality and better semantic alignment with the input instructions. Qualitative comparisons in Fig. 5 further demonstrate that LASAGNA produces superior inter-layer coherence and faithfully preserves visual effects across layers. In contrast, competing models often generate inconsistent compositions or fail to maintain alignment between foregrounds and backgrounds. Moreover, by generating physically grounded visual effects in the foreground layers, LASAGNA enables direct post-generation editing and recomposition, which are not supported by existing methods. Additionally, we evaluate our model on the public benchmarks ImgEdit-

Table 4. **Comparison with general models for layer generation.** Results for models marked with \* are obtained using their respective expert models rather than a single unified model. Specifically, for the FG\_Gen and BG\_Gen tasks, we use the FLUX.1-Fill-dev, Qwen-Image-Edit-2509, and gpt-image-1[high] editing models, respectively. For the All\_Gen task, we use the FLUX.1-schnell, Qwen-Image, and gpt-image-1[high] models as text-to-image models, respectively.

Model	# Params	FG_Gen			BG_Gen			Text2All					
		Cond Image	CFID ↓	FID ↓	GPT Score ↑	Cond Image	CFID ↓	FID ↓	GPT Score ↑	Cond Image	CFID ↓	FID ↓	GPT Score ↑
gpt-image-1[high]*	—	BG	20.3	116.9	8.8	FG	20.3	115.2	8.9	None	25.6	130.8	7.1
FLUX.1*	12B	BG, Mask	10.0	79.6	8.9	FG, Mask	16.1	105.9	8.5	None	22.7	131.1	6.0
Qwen-Image-Edit*	20B	BG, Mask	12.1	92.5	9.0	FG, Mask	15.1	101.2	7.9	None	24.9	131.5	5.7
<b>Ours</b>	2B	BG, Mask	<b>9.7</b>	<b>72.0</b>	<b>9.3</b>	FG, Mask	<b>14.1</b>	<b>98.6</b>	<b>9.0</b>	Mask	<b>16.9</b>	<b>115.8</b>	<b>7.6</b>

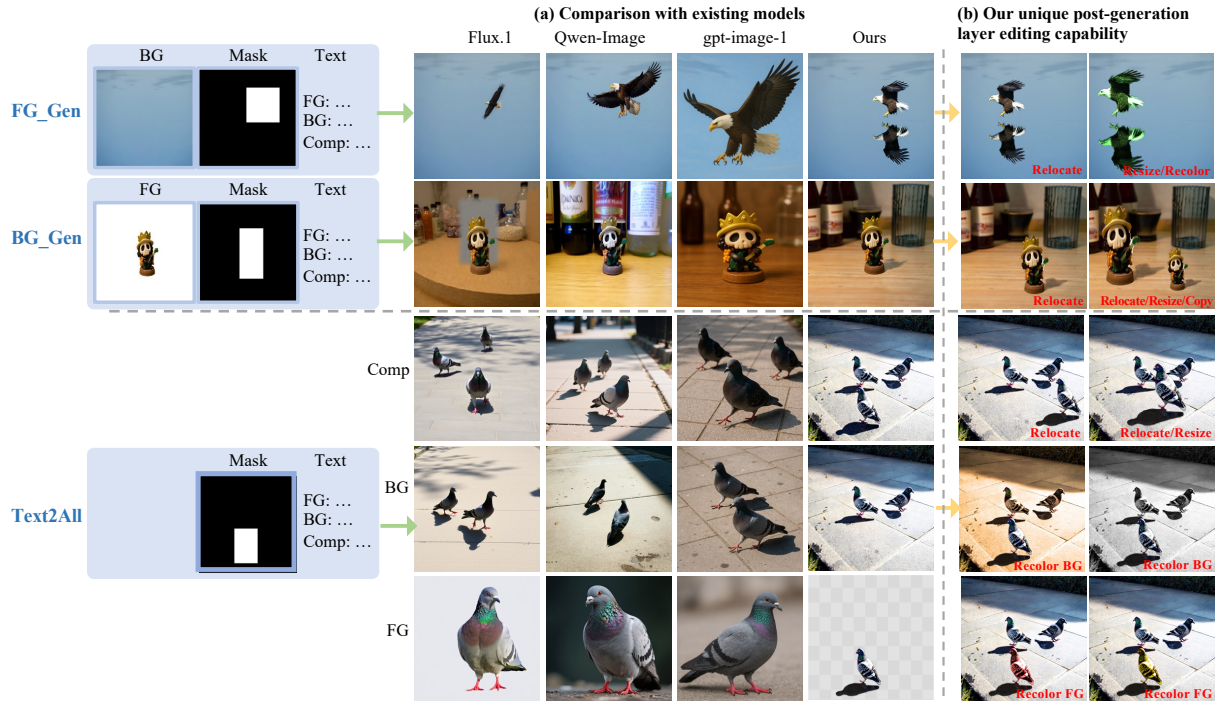


Figure 5. **Layer generation compared with state-of-the-art image generation and editing models.** We compare LASAGNA with Flux.1 [18, 24], Qwen-Image-Edit [53], and gpt-image-1[High] [31]. **(a)** Across three distinct generation tasks, LASAGNA consistently achieves superior inter-layer coherence and consistency. In contrast, competing models often fail to maintain these properties. **(b)** Moreover, by generating foregrounds with faithfully preserved visual effects, LASAGNA enables diverse post-generation editing operations on individual layers directly—a capability not supported by existing models.

Bench [58] and GenEval [15] (see Appendix).

### 4.3. Layer Generation vs Expert Model

We further compare LASAGNA with the LayerDiffuse [61], a prior work specifically designed for layered image generation through multiple expert modes. However, LayerDiffuse relies on separate, independently trained models for each task, limiting its controllability and consistency across layers. As shown in Table 5, LASAGNA significantly outperforms LayerDiffuse across all three generation modes in terms of CLIP-FID, confirming the effectiveness of our unified framework in producing coherent and semantically faithful results across diverse generation settings. Qualitative comparisons in Fig. 6 highlight these improvements. Foregrounds generated by LayerDiffuse often appear centered and lack positional diversity due to absence of explicit spatial constraints. The model

Table 5. **Comparison with LayerDiffuse [61] for layer generation.** Each cell reports CLIP-FID (↓).

Model	FG_Gen		BG_Gen		Text2All		
	Comp.	FG	Comp.	BG	FG	Comp.	BG
LayerDiffuse [61]	42.0	43.8	43.2	43.1	45.2	46.0	48.2
<b>LASAGNA</b>	<b>13.4</b>	<b>37.3</b>	<b>21.0</b>	<b>25.6</b>	<b>25.5</b>	<b>26.2</b>	<b>35.8</b>

also frequently fails to clearly separate foreground and background regions and struggles to represent all described entities when given complex captions. In contrast, LASAGNA produces spatially controlled, semantically complete, and visually coherent results across all generation modes.

### 4.4. Layer Editing with Visual Effects

To further quantify the value of explicit layer representations with visual effects for controllable image edit-

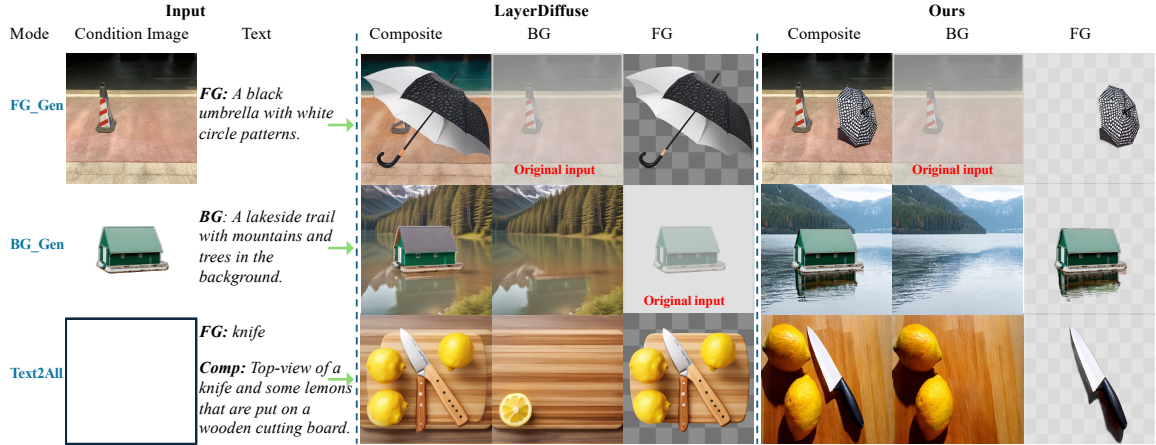


Figure 6. **Layer generation compared with LayerDiffuse [61]**. In FG\_Gen, our model produces object with appropriate size and position, along with realistic shadows consistent with the background. In BG\_Gen and Text2All, our model produces visually consistent results across all layers. Furthermore, it can generate new foregrounds with corresponding visual effects, enabling flexible and realistic post-editing.

ing, we evaluate three editing paradigms, comparing LASAGNA with Qwen-Image-Edit-2509:

1. *Instruct editing*: Prompt Qwen-Image-Edit-2509 to directly edit the image based on the textual input.
2. *Layer editing*: Use a segmentation model [30] to extract the target object, then edit the object layer explicitly (e.g., programmatically modifying its RGB values or spatial coordinates).
3. *Layer editing with visual effects*: Perform the same explicit object-layer editing as above, while additionally incorporating the visual effects (e.g., shadows and reflections) generated by LASAGNA.

We benchmark these three approaches on recoloring, spatial editing, and complex compositional editing tasks. For recoloring, we define seven random color transformation operations. For spatial editing, we randomly select a movement direction (up, down, left, or right) and apply one of three displacement magnitudes (20%, 30%, or 50%). For compositional editing, we randomly combine recoloring and spatial editing to test multi-factor control. All evaluations are conducted automatically to ensure objective and reproducible comparison across methods.

As shown in Table 6, *Layer editing* already outperforms *Instruct editing* across all editing goals, achieving higher fidelity and spatial consistency. *Layer editing with visual effects* achieves the best overall performance with substantial gains in perceptual realism and physical plausibility. Qualitative comparisons in Fig. 7 further highlight these differences. *Instruct editing* often introduces unintended global changes (e.g., altered background tones during recoloring) and struggles to achieve precise spatial edits. In contrast, *Layer editing* enables fine-grained spatial manipulation while preserving object identity, which is critical for user-driven image editing applications. Finally, *Layer editing with visual effects* produces the most visually coherent and realistic results, generating shadows and reflections that are physically consistent with the sur-

Table 6. **Comparison with Qwen [53] for layer editing.** R: recolor; M: movement; C: joint recolor+movement.

Method	R	M	C
	CLIP-FID/FID	CLIP-FID/FID	CLIP-FID/FID
Instr. (Qwen)	13.2/102.9	13.4/101.4	15.8/110.8
Layer (Qwen)	9.5/88.8	8.5/83.6	8.8/86.9
Layer+VE (Ours)	<b>8.3/71.7</b>	<b>6.5/68.4</b>	<b>6.4/71.1</b>

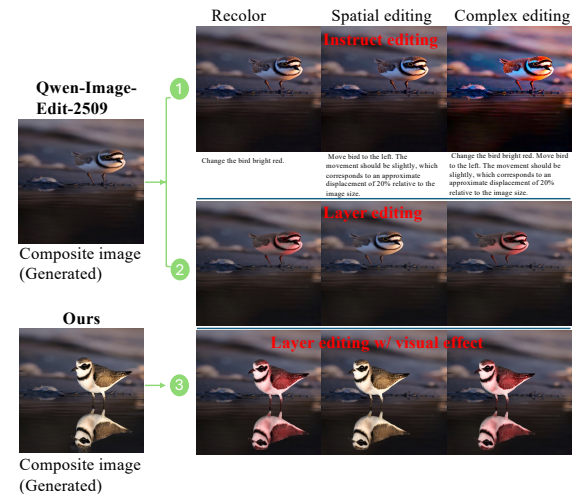


Figure 7. **Layer editing with visual effects.** We demonstrate the benefits of explicit layer representations with visual effects by comparing three paradigms: *Instruct Editing*, *Layer Editing*, and *Layer Editing with Visual Effects* (LASAGNA). Across recoloring, spatial, and compositional editing tasks, the lack of explicit layer representations makes *Instruct Editing* prone to unintended changes and less responsive to spatial instructions, while *Layer Editing with Visual Effects* yields more coherent and photorealistic results.

rounding scene. These results confirm that explicitly modeling layered representations with physically grounded visual effects is crucial for achieving realistic, consistent, and controllable image manipulation.

Table 7. **Ablation study.** Each cell reports **CLIP-FID / FID** ( $\downarrow$ ). Training with LASAGNA-48K improves over the internal-only variant, confirming its benefit. The instruction-based setting yields comparable results, showing robustness to language variation. The unified model outperforms single-task models, indicating synergy across generation modes.

Ablation	FG_Gen		BG_Gen			Text2All		
	Composite	FG	Composite	BG	FG	Composite	BG	FG
Internal data	11.3/79.7	28.9/155.9	15.9/102.9	17.8/134.0	22.5/145.2	19.6/120.4	18.1/136.2	28.8/158.0
Instruction	10.6/77.1	27.4/153.1	15.2/107.0	17.2/134.8	<b>22.6</b> /140.9	18.0/119.5	<b>16.8</b> /134.3	<b>26.6</b> /152.5
Separate task	11.0/79.7	28.4/156.7	15.6/104.1	17.8/133.6	37.2/142.0	19.2/119.6	18.4/133.4	28.6/153.3
LASAGNA	<b>10.3/75.9</b>	<b>27.3/151.8</b>	<b>14.6/102.9</b>	<b>16.8/132.5</b>	22.7/139.3	<b>17.8/119.4</b>	17.1/129.3	28.1/150.3

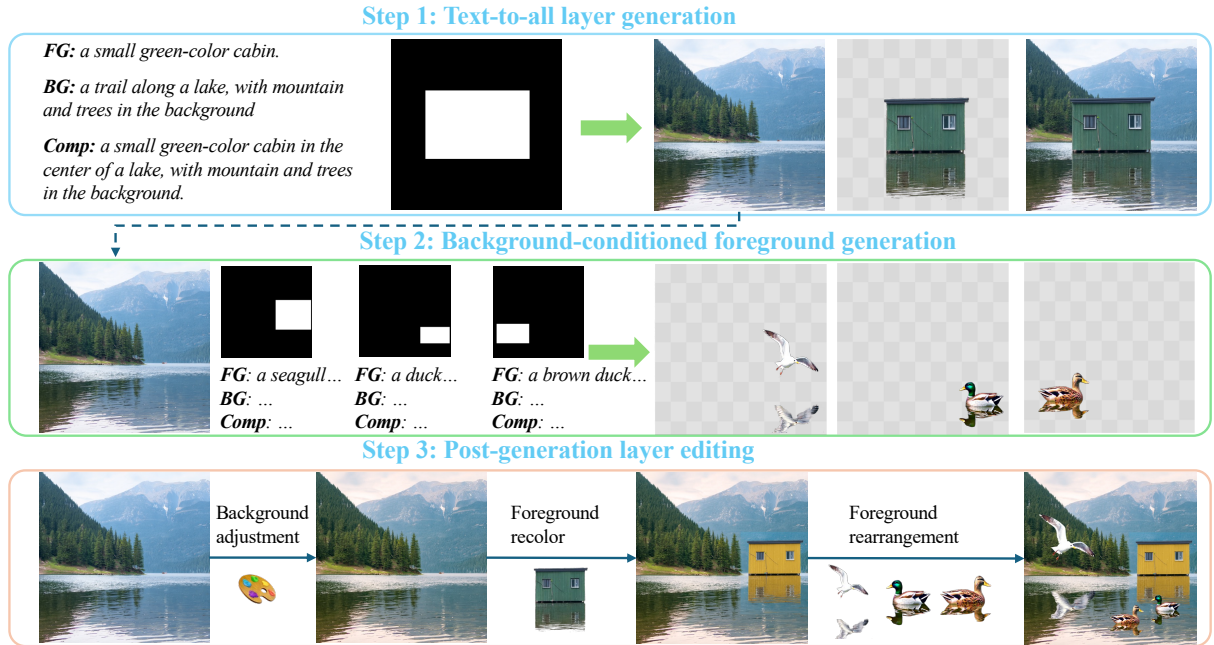


Figure 8. **Diverse creative applications driven by our model.** We leverage both Text2All and FG\_Gen modes to jointly guide the synthesis process, unlocking a broader range of editing possibilities and producing diverse, visually appealing results.

## 4.5. Ablations

We ablate our design choices in Table 7, ensuring fair and interpretable comparisons and highlighting the effectiveness of our complete LASAGNA framework. Comparing the model variant trained solely on internal data with LASAGNA, which is trained on the same internal data augmented with our public LASAGNA-48K, we observe consistent performance gains across all generation modes. This demonstrates the effectiveness and value of the newly proposed LASAGNA-48K. To examine the impact of language formulation, we convert the captions into instruction-based prompts. The resulting variant achieves comparable or slightly lower performance than LASAGNA, indicating that our framework is robust to different language input formats. We further train three independent models, each dedicated to a single generation mode. Unified LASAGNA still achieves superior performance, suggesting that joint training enables beneficial knowledge sharing and synergy across the different generation tasks.

## 4.6. Creative applications

Our framework supports generating multiple layers with realistic virtual effects under three different generation modes, enabling natural post-generation layer editing, as shown in Fig. 1 and Fig. 5. In this section, we further demonstrate that, benefiting from the highly consistent and visually coherent results across different modes, our framework allows flexible cross-mode collaborative editing, unlocking a broader range of creative possibilities. As illustrated in Fig. 8, combining the Text2All and FG\_Gen modes yields diverse and harmonized editing outcomes.

## 5. Conclusion

We present LASAGNA, a unified framework for controllable image editing via explicit layer representation with visual effects. We introduce LASAGNA-48K, the first layer dataset with grounded visual effects, and LASAGNA BENCH, the first public benchmark for layer editing. Our experiments establish LASAGNA as a new state-of-the-art in controllable layer generation. Despite these advances, LASAGNA still has several limi-

tations: it currently focuses on single-object layer generation and does not yet support generating coherent layered representations for multiple interacting objects in a single pass. Future work will explore lifting these constraints by enabling multi-object layered generation and incorporating finer-grained control over dynamic scene behaviors.

## References

- [1] Shuai Bai, Keqin Chen, Xuejing Liu, Jialin Wang, Wenbin Ge, Sibo Song, Kai Dang, Peng Wang, Shijie Wang, Jun Tang, et al. Qwen2. 5-vl technical report. *arXiv preprint arXiv:2502.13923*, 2025. 4
- [2] James Betker, Gabriel Goh, Li Jing, Tim Brooks, Jianfeng Wang, Linjie Li, Long Ouyang, Juntang Zhuang, Joyce Lee, Yufei Guo, et al. Improving image generation with better captions. *OpenAI blog*, 2023. 2
- [3] Tim Brooks, Aleksander Holynski, and Alexei A Efros. Instructpix2pix: Learning to follow image editing instructions. In *Proceedings of the IEEE/CVF conference on computer vision and pattern recognition*, pages 18392–18402, 2023. 1
- [4] Junsong Chen, Chongjian Ge, Enze Xie, Yue Wu, Lewei Yao, Xiaozhe Ren, Zhongdao Wang, Ping Luo, Huchuan Lu, and Zhenguo Li. Pixart-sigma: Weak-to-strong training of diffusion transformer for 4k text-to-image generation. In *ECCV*, 2024. 2
- [5] Xiaokang Chen, Chengyue Wu, Zhiyu Wu, Yiyang Ma, Xingchao Liu, Zizheng Pan, Wen Liu, Zhenda Xie, Xingkai Yu, Chong Ruan, and Ping Luo. Janus-pro: Unified multimodal understanding and generation with data and model scaling. *arXiv preprint arXiv:2501.17811*, 2025. 2
- [6] Xi Chen, Zhifei Zhang, He Zhang, Yuqian Zhou, Soo Ye Kim, Qing Liu, Yijun Li, Jianming Zhang, Nanxuan Zhao, Yilin Wang, et al. Unireal: Universal image generation and editing via learning real-world dynamics. In *Proceedings of the Computer Vision and Pattern Recognition Conference*, pages 12501–12511, 2025. 2, 3
- [7] Zhe Chen, Weiyun Wang, Yue Cao, Yangzhou Liu, Zhangwei Gao, Erfei Cui, Jinguo Zhu, Shenglong Ye, Hao Tian, Zhaoyang Liu, et al. Expanding performance boundaries of open-source multimodal models with model, data, and test-time scaling. *arXiv preprint arXiv:2412.05271*, 2024. 4
- [8] Yusuf Dalva, Yijun Li, Qing Liu, Nanxuan Zhao, Jianming Zhang, Zhe Lin, and Pinar Yanardag. Layerfusion: Harmonized multi-layer text-to-image generation with generative priors. *arXiv preprint arXiv:2412.04460*, 2024. 2, 3, 5
- [9] Chaorui Deng, Deyao Zhu, Kunchang Li, Chenhui Gou, Feng Li, Zeyu Wang, Shu Zhong, Weihao Yu, Xiaonan Nie, Ziang Song, et al. Emerging properties in unified multimodal pretraining. *arXiv preprint arXiv:2505.14683*, 2025. 1, 2
- [10] Patrick Esser, Sumith Kulal, Andreas Blattmann, Rahim Entezari, Jonas Müller, Harry Saini, Yam Levi, Dominik Lorenz, Axel Sauer, Frederic Boesel, et al. Scaling rectified flow transformers for high-resolution image synthesis. In *ICML*, 2024. 2
- [11] Patrick Esser, Sumith Kulal, Andreas Blattmann, Rahim Entezari, Jonas Müller, Harry Saini, Yam Levi, Dominik Lorenz, Axel Sauer, Frederic Boesel, et al. Scaling rectified flow transformers for high-resolution image synthesis. In *Forty-first international conference on machine learning*, 2024. 1, 2, 3
- [12] Alessandro Fontanella, Petru-Daniel Tudosiu, Yongxin Yang, Shifeng Zhang, and Sarah Parisot. Generating compositional scenes via text-to-image rgba instance generation. *Advances in Neural Information Processing Systems*, 37:43864–43893, 2024. 3
- [13] Shixuan Gao, Pingping Zhang, Tianyu Yan, and Huchuan Lu. Multi-scale and detail-enhanced segment anything model for salient object detection. In *Proceedings of the 32nd ACM International Conference on Multimedia*, pages 9894–9903, 2024. 4
- [14] Yuying Ge, Sijie Zhao, Jinguo Zhu, Yixiao Ge, Kun Yi, Lin Song, Chen Li, Xiaohan Ding, and Ying Shan. Seed-x: Multimodal models with unified multi-granularity comprehension and generation. *arXiv preprint arXiv:2404.14396*, 2024. 2
- [15] Dhruba Ghosh, Hannaneh Hajishirzi, and Ludwig Schmidt. Geneval: An object-focused framework for evaluating text-to-image alignment. *Advances in Neural Information Processing Systems*, 36:52132–52152, 2023. 6, 1, 2
- [16] Martin Heusel, Hubert Ramsauer, Thomas Unterthiner, Bernhard Nessler, and Sepp Hochreiter. Gans trained by a two time-scale update rule converge to a local nash equilibrium. *Advances in neural information processing systems*, 30, 2017. 5
- [17] Dingbang Huang, Wenbo Li, Yifei Zhao, Xinyu Pan, Yanhong Zeng, and Bo Dai. Psdiffusion: Harmonized multi-layer image generation via layout and appearance alignment. *arXiv preprint arXiv:2505.11468*, 2025. 2, 3, 5
- [18] Hugging Face. Flux family models. <https://huggingface.co/docs/diffusers/main/en/api/pipelines/flux>, 2025. 5, 6
- [19] Xuan Ju, Xian Liu, Xiantao Wang, Yuxuan Bian, Ying Shan, and Qiang Xu. Brushnet: A plug-and-play image inpainting model with decomposed dual-branch diffusion. In *European Conference on Computer Vision*, pages 150–168. Springer, 2024. 3
- [20] Kyoungkook Kang, Gyujin Sim, Geonung Kim, Donguk Kim, Seungho Nam, and Sunghyun Cho. Layeringdiff: Layered image synthesis via generation, then disassembly with generative knowledge. *arXiv preprint arXiv:2501.01197*, 2025. 3
- [21] Bingxin Ke, Kevin Qu, Tianfu Wang, Nando Metzger, Shengyu Huang, Bo Li, Anton Obukhov, and Konrad Schindler. Marigold: Affordable adaptation of diffusion-based image generators for image analysis. *arXiv preprint arXiv:2505.09358*, 2025. 4
- [22] Alexander Kirillov, Eric Mintun, Nikhila Ravi, Hanzi Mao, Chloe Rolland, Laura Gustafson, Tete Xiao, Spencer Whitehead, Alexander C Berg, Wan-Yen Lo, et al. Segment anything. In *Proceedings of the IEEE/CVF international conference on computer vision*, pages 4015–4026, 2023. 3
- [23] Black Forest Labs. Flux, 2024. 2
- [24] Black Forest Labs, Stephen Batifol, Andreas Blattmann, Frederic Boesel, Saksham Consul,

Cyril Diagne, Tim Dockhorn, Jack English, Zion English, Patrick Esser, et al. Flux. 1 kontext: Flow matching for in-context image generation and editing in latent space. *arXiv preprint arXiv:2506.15742*, 2025. 1, 2, 3, 5, 6

[25] Bin Lin, Zongjian Li, Xinhua Cheng, Yuwei Niu, Yang Ye, Xianyi He, Shanghai Yuan, Wangbo Yu, Shaodong Wang, Yunyang Ge, et al. Uniworld: High-resolution semantic encoders for unified visual understanding and generation. *arXiv preprint arXiv:2506.03147*, 2025. 1

[26] Tsung-Yi Lin, Michael Maire, Serge Belongie, James Hays, Pietro Perona, Deva Ramanan, Piotr Dollár, and C Lawrence Zitnick. Microsoft coco: Common objects in context. In *European conference on computer vision*, pages 740–755. Springer, 2014. 4, 5

[27] Yaron Lipman, Ricky TQ Chen, Heli Ben-Hamu, Maximilian Nickel, and Matt Le. Flow matching for generative modeling. *arXiv preprint arXiv:2210.02747*, 2022. 3

[28] Hao Liu, Wilson Yan, Matei Zaharia, and Pieter Abbeel. World model on million-length video and language with ringattention. *arXiv preprint arXiv:2402.08268*, 2024. 2

[29] Shiyu Liu, Yucheng Han, Peng Xing, Fukun Yin, Rui Wang, Wei Cheng, Jiaqi Liao, Yingming Wang, Hong-hao Fu, Chunrui Han, et al. Step1x-edit: A practical framework for general image editing. *arXiv preprint arXiv:2504.17761*, 2025. 2, 1

[30] Yuqi Liu, Bohao Peng, Zhisheng Zhong, Zihao Yue, Fanbin Lu, Bei Yu, and Jiaya Jia. Seg-zero: Reasoning-chain guided segmentation via cognitive reinforcement. *arXiv preprint arXiv:2503.06520*, 2025. 7

[31] OpenAI. Gpt image 1. <https://platform.openai.com/docs/models/gpt-image-1>, 2025. Accessed: 2025-11-13. 5, 6

[32] Xichen Pan, Satya Narayan Shukla, Aashu Singh, Zhiukai Zhao, Shlok Kumar Mishra, Jialiang Wang, Zhiyang Xu, Jiahai Chen, Kunpeng Li, Felix Juefei-Xu, Ji Hou, and Saining Xie. Transfer between modalities with metaqueries. *arXiv preprint arXiv:2504.06256*, 2025. 2

[33] Gaurav Parmar, Richard Zhang, and Jun-Yan Zhu. On aliased resizing and surprising subtleties in gan evaluation. In *CVPR*, 2022. 5

[34] William Peebles and Saining Xie. Scalable diffusion models with transformers. In *Proceedings of the IEEE/CVF International Conference on Computer Vision*, pages 4195–4205, 2023. 3

[35] Dustin Podell, Zion English, Kyle Lacey, Andreas Blattmann, Tim Dockhorn, Jonas Müller, Joe Penna, and Robin Rombach. Sdxl: Improving latent diffusion models for high-resolution image synthesis. *arXiv preprint arXiv:2307.01952*, 2023. 1, 2, 3

[36] Dustin Podell, Zion English, Kyle Lacey, Andreas Blattmann, Tim Dockhorn, Jonas Müller, Joe Penna, and Robin Rombach. Sdxl: Improving latent diffusion models for high-resolution image synthesis. In *ICLR*, 2024. 2

[37] Liao Qu, Huichao Zhang, Yiheng Liu, Xu Wang, Yi Jiang, Yiming Gao, Hu Ye, Daniel K Du, Zehuan Yuan, and Xinglong Wu. Tokenflow: Unified image tokenizer for multimodal understanding and generation. *arXiv preprint arXiv:2412.03069*, 2024. 2

[38] Colin Raffel, Noam Shazeer, Adam Roberts, Katherine Lee, Sharan Narang, Michael Matena, Yanqi Zhou, Wei Li, and Peter J Liu. Exploring the limits of transfer learning with a unified text-to-text transformer. *Journal of machine learning research*, 21(140):1–67, 2020. 3

[39] Aditya Ramesh, Mikhail Pavlov, Gabriel Goh, Scott Gray, Chelsea Voss, Alec Radford, Mark Chen, and Ilya Sutskever. Zero-shot text-to-image generation. In *International conference on machine learning*, pages 8821–8831. Pmlr, 2021. 1, 2, 3

[40] Aditya Ramesh, Prafulla Dhariwal, Alex Nichol, Casey Chu, and Mark Chen. Hierarchical text-conditional image generation with clip latents. *arXiv preprint arXiv:2204.06125*, 2022. 2

[41] Nikhila Ravi, Valentin Gabeur, Yuan-Ting Hu, Ronghang Hu, Chaitanya Ryali, Tengyu Ma, Haitham Khedr, Roman Rädle, Chloe Rolland, Laura Gustafson, et al. Sam 2: Segment anything in images and videos. *arXiv preprint arXiv:2408.00714*, 2024. 3

[42] Tianhe Ren, Shilong Liu, Ailing Zeng, Jing Lin, Kun-chang Li, He Cao, Jiayu Chen, Xinyu Huang, Yukang Chen, Feng Yan, et al. Grounded sam: Assembling open-world models for diverse visual tasks. *arXiv preprint arXiv:2401.14159*, 2024. 3

[43] Robin Rombach, Andreas Blattmann, Dominik Lorenz, Patrick Esser, and Björn Ommer. High-resolution image synthesis with latent diffusion models. In *Proceedings of the IEEE/CVF conference on computer vision and pattern recognition*, pages 10684–10695, 2022. 1, 2, 3

[44] Chameleon Team. Chameleon: Mixed-modal early-fusion foundation models. *arXiv preprint arXiv:2405.09818*, 2024. 2

[45] Petru-Daniel Tudosiu, Yongxin Yang, Shifeng Zhang, Fei Chen, Steven McDonagh, Gerasimos Lampouras, Ignacio Iacobacci, and Sarah Parisot. Mulan: A multi layer annotated dataset for controllable text-to-image generation. In *Proceedings of the IEEE/CVF Conference on Computer Vision and Pattern Recognition*, pages 22413–22422, 2024. 2, 3, 4, 5

[46] Unsplash. Unsplash: Free high-resolution photos. <https://unsplash.com/>. 5

[47] Chunwei Wang, Guansong Lu, Junwei Yang, Runhui Huang, Jianhua Han, Lu Hou, Wei Zhang, and Hang Xu. Illume: Illuminating your llms to see, draw, and self-enhance. *arXiv preprint arXiv:2412.06673*, 2024. 2

[48] Tianyu Wang, Xiaowei Hu, Pheng-Ann Heng, and Chi-Wing Fu. Instance shadow detection with a single-stage detector. *IEEE transactions on pattern analysis and machine intelligence*, 45(3):3259–3273, 2022. 4, 5

[49] Xinlong Wang, Xiaosong Zhang, Zhengxiong Luo, Quan Sun, Yufeng Cui, Jinsheng Wang, Fan Zhang, Yueze Wang, Zhen Li, Qiying Yu, et al. Emu3: Next-token prediction is all you need. *arXiv preprint arXiv:2409.18869*, 2024. 2

[50] Runpu Wei, Zijin Yin, Shuo Zhang, Lanxiang Zhou, Xueyi Wang, Chao Ban, Tianwei Cao, Hao Sun, Zhongjiang He, Kongming Liang, et al. Omnieraser: Remove objects and their effects in images with paired

video-frame data. *arXiv preprint arXiv:2501.07397*, 2025. 3

[51] Daniel Winter, Matan Cohen, Shlomi Fruchter, Yael Pritch, Alex Rav-Acha, and Yedid Hoshen. Object-drop: Bootstrapping counterfactuals for photorealistic object removal and insertion. In *European Conference on Computer Vision*, pages 112–129. Springer, 2024. 3, 5

[52] Chengyue Wu, Xiaokang Chen, Zhiyu Wu, Yiyang Ma, Xingchao Liu, Zizheng Pan, Wen Liu, Zhenda Xie, Xingkai Yu, Chong Ruan, and Ping Luo. Janus: Decoupling visual encoding for unified multimodal understanding and generation. *arXiv preprint arXiv:2410.13848*, 2024. 2

[53] Chenfei Wu, Jiahao Li, Jingren Zhou, Junyang Lin, Kaiyuan Gao, Kun Yan, Sheng-ming Yin, Shuai Bai, Xiao Xu, Yilei Chen, et al. Qwen-image technical report. *arXiv preprint arXiv:2508.02324*, 2025. 1, 2, 3, 5, 6, 7

[54] Chenyuan Wu, Pengfei Zheng, Ruiran Yan, Shitao Xiao, Xin Luo, Yueze Wang, Wanli Li, Xiyuan Jiang, Yexin Liu, Junjie Zhou, et al. Omnipgen2: Exploration to advanced multimodal generation. *arXiv preprint arXiv:2506.18871*, 2025. 1

[55] Jinheng Xie, Weijia Mao, Zechen Bai, David Junhao Zhang, Weihao Wang, Kevin Qinghong Lin, Yuchao Gu, Zhijie Chen, Zhenheng Yang, and Mike Zheng Shou. Show-o: One single transformer to unify multimodal understanding and generation. *arXiv preprint arxiv:2408.12528*, 2024. 2

[56] Jinrui Yang, Qing Liu, Yijun Li, Soo Ye Kim, Daniil Pakhomov, Mengwei Ren, Jianming Zhang, Zhe Lin, Cihang Xie, and Yuyin Zhou. Generative image layer decomposition with visual effects. In *Proceedings of the Computer Vision and Pattern Recognition Conference*, pages 7643–7653, 2025. 3, 4, 5

[57] Siwei Yang, Mude Hui, Bingchen Zhao, Yuyin Zhou, Nataniel Ruiz, and Cihang Xie. Complexedit: Cot-like instruction generation for complexity-controllable image editing benchmark. *arXiv preprint arXiv:2504.13143*, 2025. 5, 1

[58] Yang Ye, Xianyi He, Zongjian Li, Bin Lin, Shenghai Yuan, Zhiyuan Yan, Bohan Hou, and Li Yuan. Imgedit: A unified image editing dataset and benchmark. *arXiv preprint arXiv:2505.20275*, 2025. 6, 1

[59] Qifan Yu, Wei Chow, Zhongqi Yue, Kaihang Pan, Yang Wu, Xiaoyang Wan, Juncheng Li, Siliang Tang, Hanwang Zhang, and Yuetong Zhuang. Anyedit: Mastering unified high-quality image editing for any idea. In *Proceedings of the Computer Vision and Pattern Recognition Conference*, pages 26125–26135, 2025. 1

[60] Kai Zhang, Lingbo Mo, Wenhui Chen, Huan Sun, and Yu Su. Magicbrush: A manually annotated dataset for instruction-guided image editing. *Advances in Neural Information Processing Systems*, 36:31428–31449, 2023. 1

[61] Lvmin Zhang and Maneesh Agrawala. Transparent image layer diffusion using latent transparency. *arXiv preprint arXiv:2402.17113*, 2024. 2, 3, 5, 6, 7

[62] Lvmin Zhang, Anyi Rao, and Maneesh Agrawala. Adding conditional control to text-to-image diffusion models. In *Proceedings of the IEEE/CVF international conference on computer vision*, pages 3836–3847, 2023. 2

[63] Richard Zhang, Phillip Isola, Alexei A Efros, Eli Shechtman, and Oliver Wang. The unreasonable effectiveness of deep features as a perceptual metric. In *Proceedings of the IEEE conference on computer vision and pattern recognition*, pages 586–595, 2018. 5

[64] Xinyang Zhang, Wentian Zhao, Xin Lu, and Jeff Chien. Text2layer: Layered image generation using latent diffusion model. *arXiv preprint arXiv:2307.09781*, 2023. 3

[65] Zechuan Zhang, Ji Xie, Yu Lu, Zongxin Yang, and Yi Yang. In-context edit: Enabling instructional image editing with in-context generation in large scale diffusion transformer. *arXiv preprint arXiv:2504.20690*, 2025. 1

[66] Haozhe Zhao, Xiaojian Shawn Ma, Liang Chen, Shuzheng Si, Ruijie Wu, Kaikai An, Peiyu Yu, Min-jia Zhang, Qing Li, and Baobao Chang. Ultraedit: Instruction-based fine-grained image editing at scale. *Advances in Neural Information Processing Systems*, 37:3058–3093, 2024. 2, 1

[67] Jixin Zhao, Shangchen Zhou, Zhouxia Wang, Peiqing Yang, and Chen Change Loy. Objectclear: Complete object removal via object-effect attention. *arXiv preprint arXiv:2505.22636*, 2025. 3

[68] Yichuan Zhong, Yapeng Tian, et al. Tp-blend: Textual-prompt attention pairing for precise object-style blending in diffusion models. *Transactions on Machine Learning Research*, 2025. 2

[69] Chunting Zhou, Lili Yu, Arun Babu, Kushal Tirumala, Michihiro Yasunaga, Leonid Shamis, Jacob Kahn, Xuezhe Ma, Luke Zettlemoyer, and Omer Levy. Transfusion: Predict the next token and diffuse images with one multi-modal model. *arXiv preprint arxiv:2408.11039*, 2024. 2

[70] Junhao Zhuang, Yanhong Zeng, Wenran Liu, Chun Yuan, and Kai Chen. A task is worth one word: Learning with task prompts for high-quality versatile image inpainting. In *European Conference on Computer Vision*, pages 195–211. Springer, 2024. 3

# Controllable Layered Image Generation for Real-World Editing

## Supplementary Material

Model	Addition	Background
MagicBrush [60]	2.84	1.75
Instruct-P2P [3]	2.45	1.44
AnyEdit [59]	3.18	2.24
UltraEdit [66]	3.44	2.83
ICEdit [65]	3.58	3.08
Step1X-Edit [29]	3.88	3.16
UniWorld-V1 [25]	3.82	2.99
BAGEL [9]	3.81	3.39
OmniGen2 [54]	3.57	3.57
Kontext-dev [24]	3.83	3.98
LASAGNA	3.86	3.32

Table 8. **Evaluation of image editing ability on ImgEdit-Bench [58].** “Addition” corresponds to FG\_Cond, and “Background” corresponds to BG\_Cond.

## 6. Comparison on Public Benchmarks

To comprehensively evaluate the ability of LASAGNA, we additionally evaluate LASAGNA on two public benchmarks: ImgEdit-Bench [58] and GenEval [15]. In ImgEdit-Bench, the “Addition” and “Background” tasks basically match our generation modes: FG\_Cond and BG\_Cond. GenEval matches our Text2All generation mode.

The results are presented in Table 8 and Table 9. All results are evaluated on the composite image. Overall, our model achieves performance competitive with state-of-the-art image editing and generation methods. Moreover, a key advantage of our approach is its ability to perform **layer generation with visual effects**, a capability not supported by existing models. The effectiveness of layer representations—and their clear benefits for subsequent editing quality—has been thoroughly validated in the main manuscript, highlighting a unique strength of our method.

## 7. More Qualitative Results from LASAGNA

As shown in Fig.9, Fig.10, and Fig. 11, we provide more results of our model under three different modes (FG\_Gen, BG\_Gen, and Text2All).

Specifically, in Fig.9 and Fig.10, for the FG\_Gen and BG\_Gen modes, we further demonstrate more flexible applications. We can fix the background and generate different foregrounds, or fix the foreground and generate different backgrounds.

## 8. More Samples from LASAGNA-48K

As shown in Fig. 12, we provide more samples from LASAGNA-48K.

## 9. More Samples from LASAGNABENCH

As shown in Fig. 13, we provide more samples from LASAGNABENCH.

## 10. Detailed Scores of the GPT Score

As shown in **Table 4** in the main manuscript, we provide the “GPT Score”, which is the average score of the instruction-following and identity-preserving metrics proposed by Complex-Edit [57]. Here, we additionally provide the original score in Table 10. We run the same prompt three times and take the average as the original score for instruction-following and identity-preserving.

## 11. Details of the Metric in Section 4.4 (Layer Editing with Visual Effects)

To illustrate the necessity of our proposed generation paradigm (Layer Editing with Visual Effects), we conduct quantitative experiments in **Section 4.4** of the main manuscript. The results show the superiority of our generation paradigm.

We compare three editing modes: *Instruct Editing*, *Layer Editing*, and *Layer Editing with Visual Effects*. For both *Layer Editing* and *Layer Editing with Visual Effects*, the foreground is represented in RGBA format, which allows us to perform programmatic, pixel-accurate modifications. This also ensures that the editing parameters remain fully consistent across the two modes.

For *Instruct Editing* mode, when performing re-color and spatial editing, we input the editing parameters from the previous Layer Editing into GPT-5. Based on the context of our question and the value of the parameter, GPT-5 generates an appropriate natural language description, as shown in the template in Fig. 14. In the subsequent Complex Editing task, we combine the two types of instructions accordingly. This helps ensure that all three types of editing perform the same actions as much as possible, thereby ensuring comparability.

## 12. Training Samples of Data Curator

In **Section 3.2**, LASAGNA-48K Dataset in the main manuscript, we demonstrate the complete data construction pipeline. The data curator is a key component in the data construction pipeline. To obtain high-quality data filtering results, we carefully annotated about 30K samples by humans, as shown in Fig. 15, to train the data curator. Each sample is a triplet data: a composite image, mask and a background without the foreground, which are input into the data curator. The

Type	Model	Single Obj.	Two Obj.	Counting	Colors	Position	Color Attri.	Overall↑
Gen. Only	PixArt- $\alpha$ [4]	0.98	0.50	0.44	0.80	0.08	0.07	0.48
	SDv2.1 [43]	0.98	0.51	0.44	0.85	0.07	0.17	0.50
	DALL-E 2 [40]	0.94	0.66	0.49	0.77	0.10	0.19	0.52
	Emu3-Gen [49]	0.98	0.71	0.34	0.81	0.17	0.21	0.54
	SDXL [36]	0.98	0.74	0.39	0.85	0.15	0.23	0.55
	DALL-E 3 [2]	0.96	0.87	0.47	0.83	0.43	0.45	0.67
	SD3-Medium [10]	0.99	0.94	0.72	0.89	0.33	0.60	0.74
	FLUX.1-dev <sup>†</sup> [23]	0.98	0.93	0.75	0.93	0.68	0.65	0.82
Unified	Chameleon [44]	-	-	-	-	-	-	0.39
	LWM [28]	0.93	0.41	0.46	0.79	0.09	0.15	0.47
	SEED-X [14]	0.97	0.58	0.26	0.80	0.19	0.14	0.49
	TokenFlow-XL [37]	0.95	0.60	0.41	0.81	0.16	0.24	0.55
	ILLUME [47]	0.99	0.86	0.45	0.71	0.39	0.28	0.61
	Janus [52]	0.97	0.68	0.30	0.84	0.46	0.42	0.61
	Transfusion [69]	-	-	-	-	-	-	0.63
	Emu3-Gen <sup>†</sup> [49]	0.99	0.81	0.42	0.80	0.49	0.45	0.66
	Show-o [55]	0.98	0.80	0.66	0.84	0.31	0.50	0.68
	Janus-Pro-7B [5]	0.99	0.89	0.59	0.90	0.79	0.66	0.80
	MetaQuery-XL <sup>†</sup> [32]	-	-	-	-	-	-	0.80
	BAGEL [9]	0.99	0.94	0.81	0.88	0.64	0.63	0.82
	BAGEL <sup>†</sup> [9]	0.98	0.95	0.84	0.95	0.78	0.77	0.88
	LASAGNA <sup>†</sup>	0.99	0.97	0.78	0.83	0.74	0.65	0.83

Table 9. **Evaluation of text-to-image generation ability on GenEval [15] benchmark.** ‘Gen. Only’ stands for an image generation model, and ‘Unified’ denotes a model that has both understanding and generation capabilities. <sup>†</sup> refer to the methods using LLM rewriter.

Table 10. **GPT scores.** “FG\_Gen” denotes background-conditioned foreground layer generation, “BG\_Gen” denotes foreground-conditioned background generation, and “Text2All” denotes text-to-all layer generation. “IF” stands for Instruction Following and “IP” for Identity Preservation. Results for models marked with \* are obtained using their respective expert models rather than a single unified model. Specifically, for the FG\_Gen and BG\_Gen tasks, we use the FLUX.1-Fill-dev, Qwen-Image-Edit-2509, and gpt-image-1[high] editing models, respectively. For the All\_Gen task, we use the FLUX.1-schnell, Qwen-Image, and gpt-image-1[high] models as text-to-image models, respectively.

Model	FG_Gen			BG_Gen			Text2All		
	IF↑	IP↑	Avg	IF↑	IP↑	Avg	IF↑	IP↑	Avg
gpt-image-1[high]*	9.77	7.88	8.8	9.84	7.95	8.9	6.95	7.26	7.1
FLUX.1*	8.32	9.46	8.9	8.43	8.48	8.5	6.46	5.61	6.0
Qwen-Image-Edit*	8.66	9.34	9.0	7.25	8.46	7.9	6.41	4.98	5.7
<b>Ours</b>	9.27	9.29	9.3	9.34	8.67	9.0	8.31	6.91	7.6

curator outputs a confidence score (between 0 and 1) indicating the probability that the background is good.

In manual annotation, we provide a binary label for each data sample. Specifically, we determine the final binary label based on the following three aspects:

- **Hole filling:** Whether the object has been successfully removed.
- **Background consistency:** Whether the removed area is consistent with the surrounding environment.
- **Visual effect:** Whether the visual effects caused by the object (e.g., shadow and reflection) have been

removed.

If **any one** of the above criteria is not met, the sample is considered a bad case. Only when all conditions are satisfied is it labeled as a good case. We highlight these unnatural regions with dashed boxes in Fig. 15. These hard negative samples ensure that, after training the data curator, the filtered data it produces consists exclusively of high-quality background images.

## Background-conditioned foreground generation

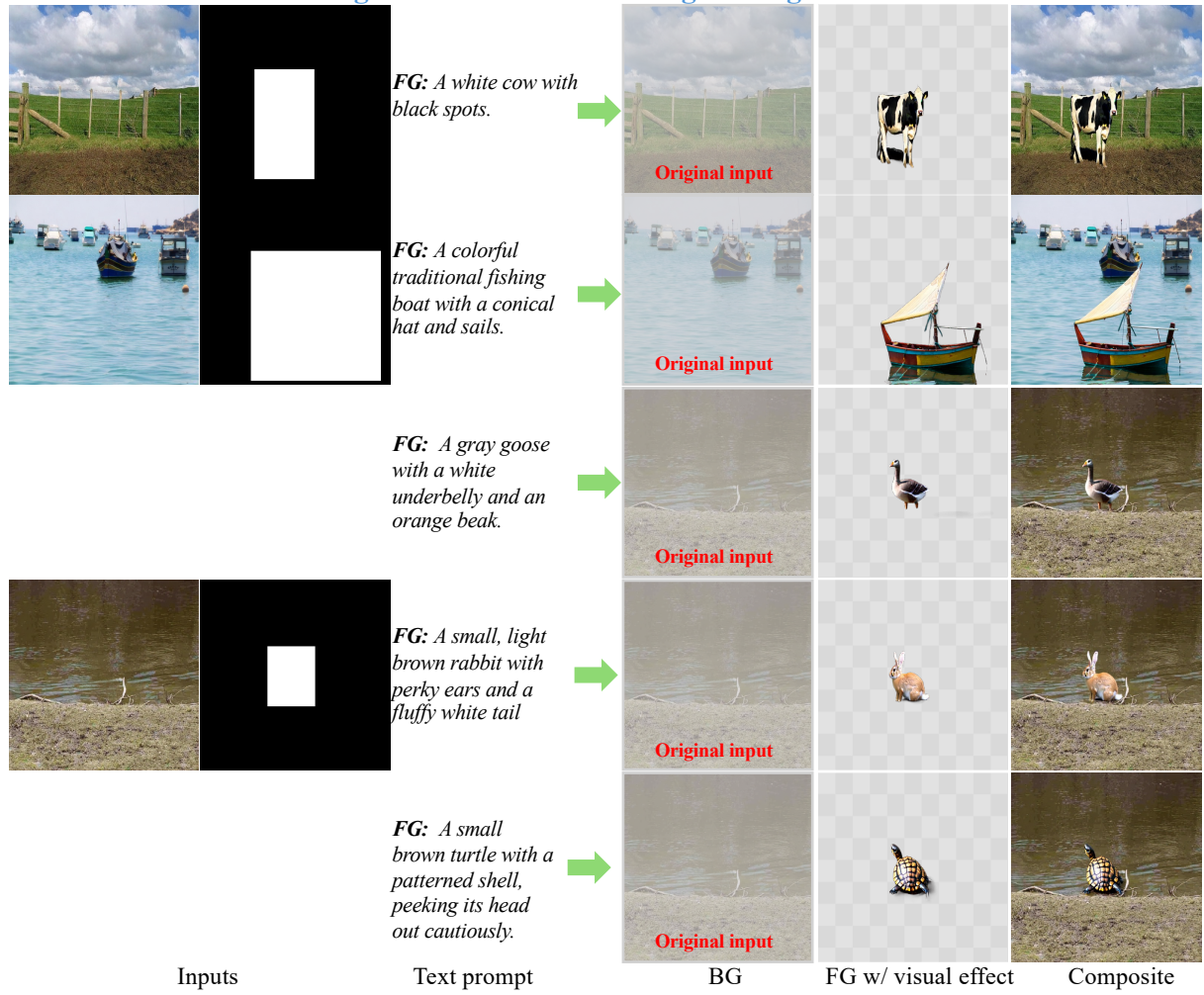


Figure 9. More results from LASAGNA under the background-conditioned foreground generation (FG\_Gen) mode.

### Foreground-conditioned background generation

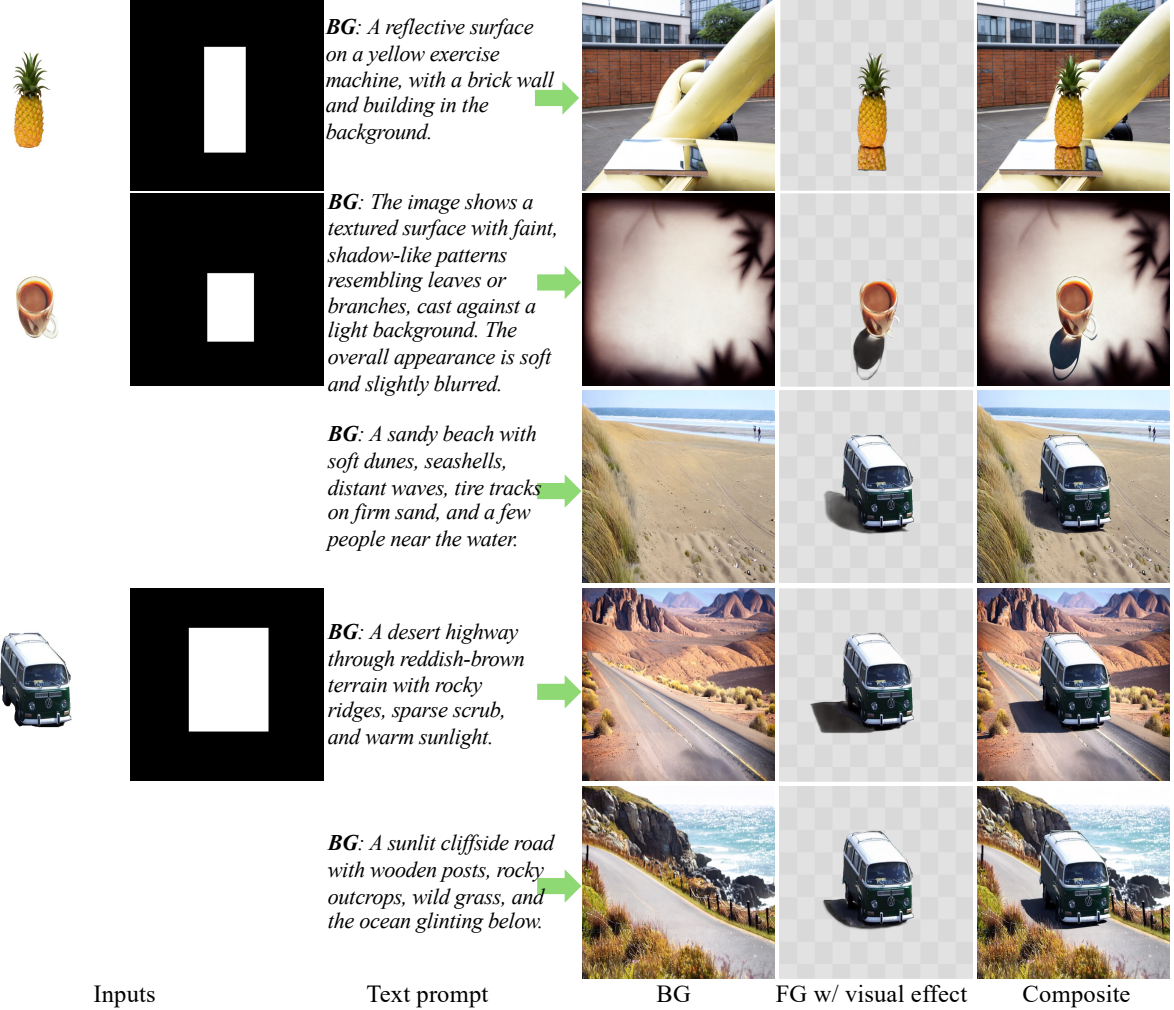


Figure 10. More results from LASAGNA under the foreground-conditioned background generation (BG\_Gen) mode.

### Text-to-all layer generation



Figure 11. More results from LASAGNA under the text-to-all layer generation (Text2All) mode.

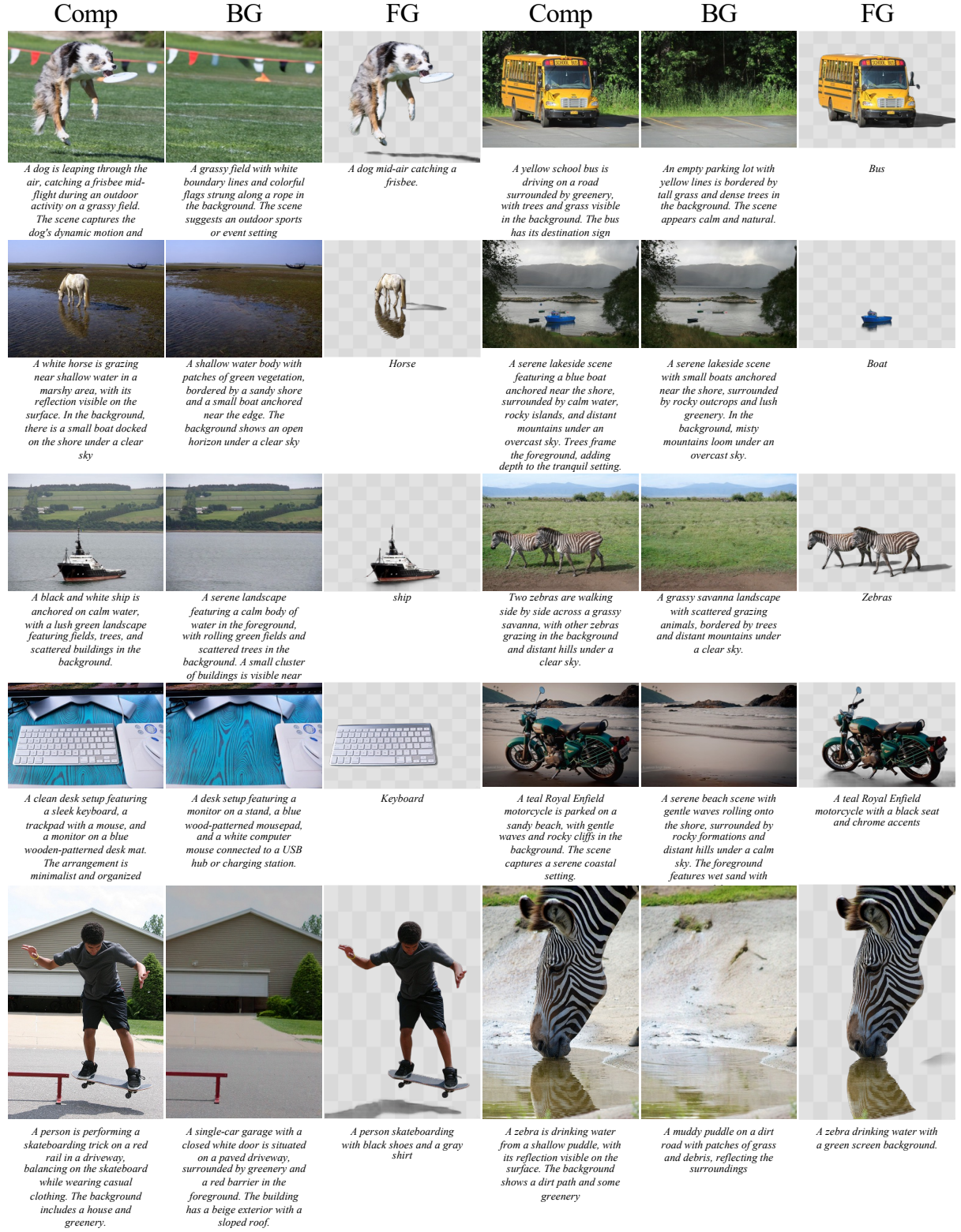


Figure 12. **More samples of LASAGNA-48K.** Each sample consists of a composite image, a clean background, and a foreground layer with visual effects, along with corresponding captions for all components.

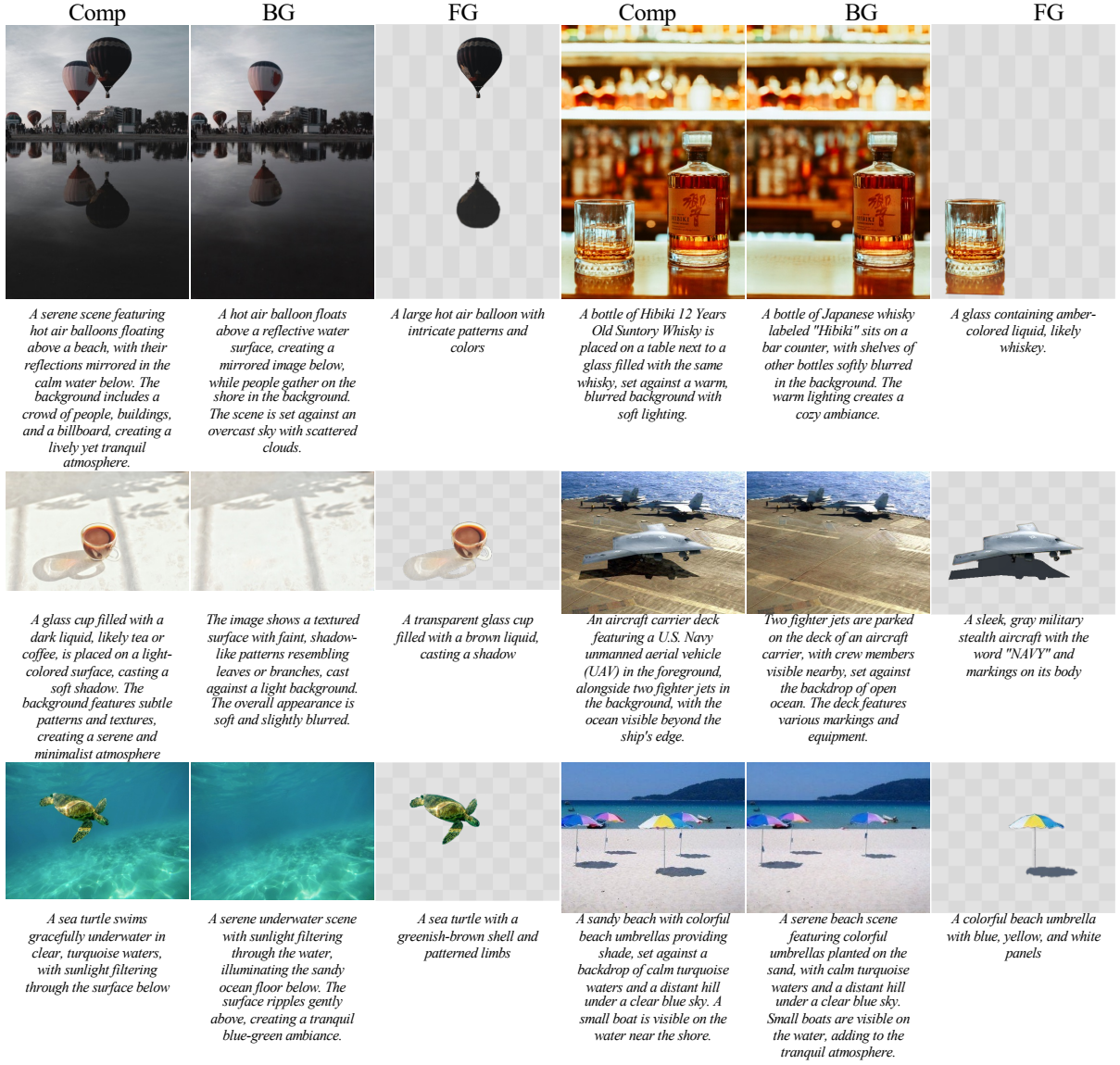


Figure 13. **More samples of LASAGNA BENCH.** Each sample consists of a composite image, a foreground layer with visual effects, and a clean background along with corresponding captions for all components. **Foreground with visual effects annotated by professional annotators. Background are decomposed by expert models or captured by camera.**

### Template of Instruction Editing

Recolor	Spatial editing
1.Red: Change the {Object} bright red.	Magnitude: {20,30,50}
2.Orange: Change the {Object} to vibrant orange.	Intensity: {slightly, moderately, significantly}
3.Yellow: Change the {Object} sunny yellow.	Direction: {to the left, to the right, upwards, downwards}
4.Green: Change the {Object} intense green.	
5.Cyan: Change the {Object} to vivid cyan.	Move {Object} {Direction}. The movement should be {Intensity}, which corresponds to an approximate displacement of {Magnitude}% relative to the image size
6.Blue: Change the {Object} deep blue.	
7.Purple: Change the {Object} rich purple.	

Figure 14. When performing instruct editing, the content within {} will be replaced by specific parameters. In spatial editing, the values of the Magnitude and Intensity parameters correspond one-to-one from left to right.

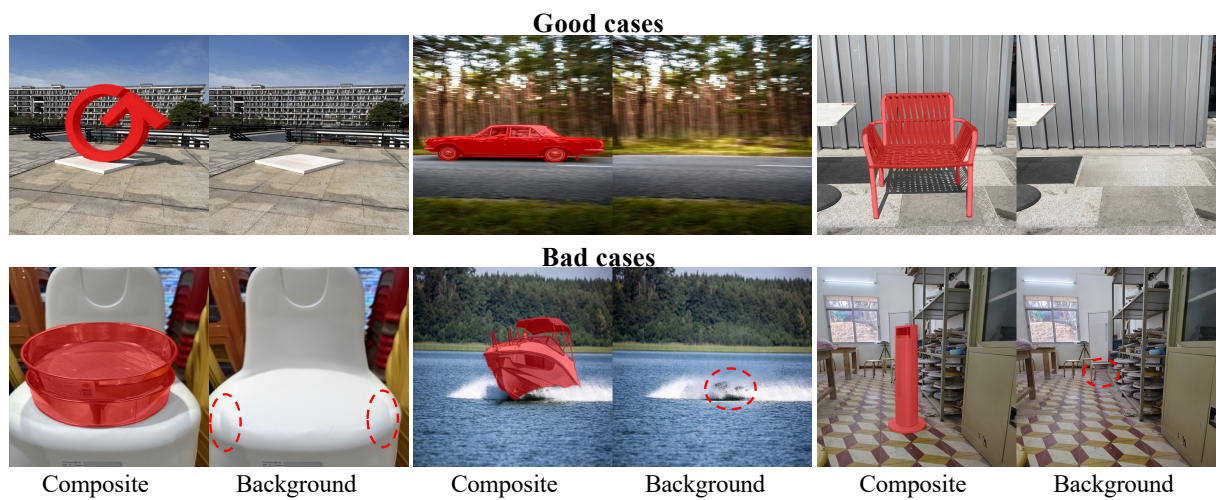


Figure 15. **Training Samples of Data Curator.** The red dashed box indicates the main problematic area in the bad cases.